

# DEVELOPMENT OF A TWIST PANTOGRAPH MECHANISM FOR ROBOTIC TELE-ECHOGRAPHY

Kohji MASUDA and Hiroaki KATO

Graduate School of Bio-Applications and Systems Engineering (BASE),  
Tokyo University of Agriculture & Technology, Japan

E-mail: k\_masuda@cc.tuat.ac.jp

**Abstract:** We have developed a twist pantograph mechanism for robotic tele-echography. We have reduced the total weight of the robot from the previous version. By introducing the inverse kinematics, three-dimensional position and angle of ultrasound probe are able to operated on body surface. Movable area, precision of the position and performance are satisfied with requirement of a diagnosis in echography. We have considered safety by detecting contact force on body surface. We have experimented and confirmed to be able to obtain echogram of remote patient by controlling the robot as physician's desire.

## Introduction

Echography is nowadays indispensable in every field of medical diagnosis because of its safety and costeffectiveness. However, a physician is required to be experienced to handle an ultrasound probe and to obtain echograms as his desire. To reproduce a technique of an expert physician, medical robots for echography have been developed[1-6] to place the ultrasound probe on patient abdomen. Their main applications aimed to a remote diagnosis of echography by controlling position and angle of the probe remotely, which is called as tele-echography. The system enables ultrasound diagnosis under a condition where a patient is apart from a physician. Though there were problems in movable area and weight in our previous robot[5,6], we have solved them by introducing a twist pantograph mechanism. We have reduced number of actuators for size reduction and compensated the necessary motion by combining motions of other parts. It enables a mobile tele-echography between an ambulance and a hospital by connecting with wireless network. In this paper we introduce a medical robot for tele-echography to be applicable in a narrow space of an emergency vehicle.

## Robot constructions and twist motion

The robot is designed to move the ultrasound probe on the human abdomen in three dimensions. It has 6 degrees of freedom and detects contact force on the body. The robot consists of pantograph, gimbals and slide parts as shown in Figure 1. The gimbals part locates in the centre of the robot and grasps the probe to rotate in pitch and yaw angle. Pantograph part has two arms which run on the rail of slide parts. The pantograph and the slide parts translate the probe in  $x$ - $z$  plane and in  $y$ -position, respectively. The roll angle of the probe is realized by combining motion of both the pantograph

and the slide parts, to twist two arms of the pantograph independently.

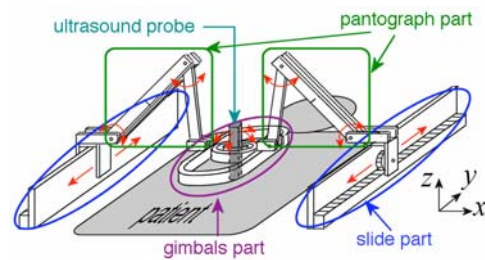


Figure 1: Construction of the twist pantograph mechanism

Other robots[2-4] for echography employed serial link mechanism with stiff joints to guarantee precise position. However, it requires heavy basement to sustain total weight of the serial link and occupies large spatial area. Thus the situation of application is limited and is not suitable to be loaded on board of a vehicle. Safety to a patient should be regarded more important than preciseness of position because resolution of mm order is not necessary for echography. By using two arms, the probe is more stabilized where single arm of the pantograph is insufficient to handle the probe by itself.

The motion of the gimbals part is equivalent to wrist of a physician. Figure 2 shows the construction of the gimbals which includes three rings. Ellipse ring is to connect two arms of the pantograph. Outer and inner rings are for pitch and yaw angle rotation, respectively. To avoid mechanical interference between actuators and rings, the axes of actuators are bent 90 degree through bevel gears. Removing an actuator for roll angle rotation from the gimbals in our previous robot[5,6], the gimbals are slimmed and the total weight of the robot reduced from 3.3 to 2.0[kg].

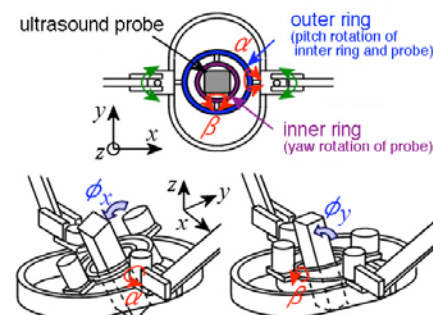


Figure 2: Construction and motion of the gimbals part

To grasp the probe in the inner ring of the gimbals, we have developed a pentagonal-shape vice as shown in Figure 3. Various types of probe can be grasped stably by using it.



Figure 3: Inner ring with the pentagonal-shape vice

Figure 4 shows the way to realize roll angle rotation of the probe by twisting each arm of the pantograph. Two arms are shifted in the opposite  $y$ -direction to tilt the arms inside. Three-dimensional rotation is possible by combining the twist motion of the pantograph with the gimbal.

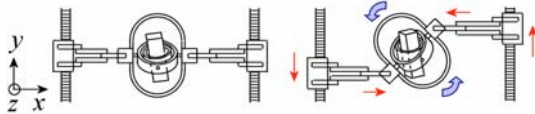


Figure 4: Twist motion of the pantograph

### Introduction of inverse kinematics

In our previous robot[5], relative position control was employed because an arm of the pantograph had an actuator only at the basements of  $O$  or  $O'$  in Figure 5. We have added more two actuators at the joints  $C$  and  $D$  to designate the coordinate of the head (the contact point to body surface) of the probe by introducing inverse kinematics.

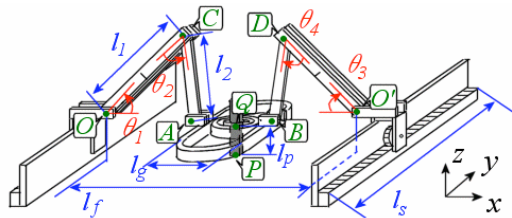


Figure 5: Definition of points, angles and lengths

Figure 5 shows the definition: the head of the probe as  $P$ , the centre point of the gimbals as  $Q$ , distance between  $P$  and  $Q$  as  $l_p$ , lengths of link as  $l_1$  and  $l_2$ , distance between two slides as  $l_g$ ,  $x$ -width of the gimbals as  $l_g$ , movable  $y$ -length of the slides as  $l_s$ , joint angles of the pantograph as  $\theta_1$ - $\theta_4$  and angles of the gimbals as  $\alpha$  and  $\beta$ . All angles should be expressed by command of the position  $P(x_p, y_p, z_p)$  and the orientation angle ( $\phi_x, \phi_y, \phi_z$ ) of the probe.

#### (a) Pivot motion

Pivot motion of the probe is necessary by touching the head of the probe on body surface which is a principal motion in actual echography. First, angles of the gimbals  $\alpha$  and  $\beta$  correspond to  $\phi_x$  and  $\phi_y$  as shown in Figure 2. Once position of the gimbals varied by the pantograph motion, the angles  $\alpha$  and  $\beta$  rotate to compensate the difference between the command and the actual angle. Figure 6 and equation (1) show the way for the pivot motion.

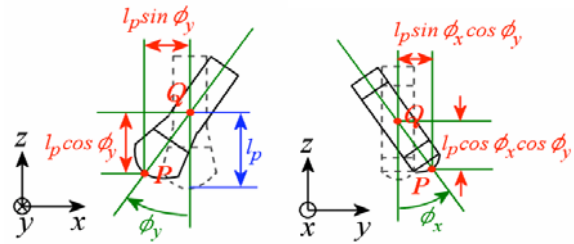


Figure 6: Pivot motion of yaw (left) and pitch angle (right)

$$\begin{pmatrix} x_Q \\ y_Q \\ z_Q \end{pmatrix} = \begin{pmatrix} x_P \\ y_P \\ z_P \end{pmatrix} + \begin{pmatrix} l_p \cos \phi_x \sin \phi_y \\ -l_p \sin \phi_x \cos \phi_y \\ l_p \cos \phi_x \cos \phi_y \end{pmatrix} \quad (1)$$

#### (b) Slide motion for roll angle rotation

To realize roll angle rotation of the probe, two arms of the pantograph shift  $\Delta y$  in the opposite direction as shown in Figure 7. Displacement of the slide is calculated from sine component of the roll angle  $\phi_z$ . Assuming the initial  $y$ -position of  $P$  as  $y_p$ ,  $y$ -position of the arms are calculated as equations (2) and (3).

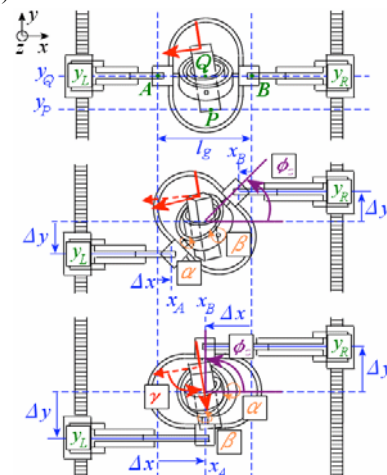


Figure 7: Roll angle rotation by twisting two arms of pantograph

$$y_L = y_p - \frac{l_g}{2} \sin \phi_z - l_p \sin \phi_x \cos \phi_y \quad (2)$$

$$y_R = y_p + \frac{l_g}{2} \sin \phi_z - l_p \sin \phi_x \cos \phi_y \quad (3)$$

#### (c) Pantograph motion for roll angle rotation

In the same time, the pantograph produce cosine component of the roll angle  $\phi_z$ . Coordinates of  $A$  and  $B$  are calculated from equations from (4) to (7).

$$x_A = x_p - \frac{l_g}{2} \cos \phi_z + l_p \sin \phi_x \cos \phi_y \quad (4)$$

$$z_A = z_p + l_p \cos \phi_x \cos \phi_y \quad (5)$$

$$x_B = x_p + \frac{l_g}{2} \cos \phi_z + l_p \sin \phi_x \cos \phi_y \quad (6)$$

$$z_B = z_p + l_p \cos \phi_x \cos \phi_y \quad (7)$$

(d) All angles in the pantograph and the gimbals

Considering all relations above, all angles of joints  $\theta_1$ - $\theta_4$  are calculated from equations from (8) to (11), where  $l_A$  and  $l_B$  are given as equations (12) and (13).

$$\theta_1 = \text{Cos}^{-1} \frac{l_1^2 - l_2^2 + l_A^2}{2l_1l_A} + \text{Tan}^{-1} \frac{z_A}{x_A} \quad (8)$$

$$\theta_2 = \text{Cos}^{-1} \frac{-l_1^2 + l_2^2 + l_A^2}{-2l_1l_A} - \text{Cos}^{-1} \frac{l_1^2 - l_2^2 + l_A^2}{2l_1l_A} \quad (9)$$

$$\theta_3 = \text{Cos}^{-1} \frac{l_1^2 - l_2^2 + l_B^2}{2l_1l_B} + \text{Tan}^{-1} \frac{z_B}{l_f - x_B} \quad (10)$$

$$\theta_4 = \text{Cos}^{-1} \frac{-l_1^2 + l_2^2 + l_B^2}{-2l_1l_B} - \text{Cos}^{-1} \frac{l_1^2 - l_2^2 + l_B^2}{2l_1l_B} \quad (11)$$

$$l_A = \sqrt{x_A^2 + z_A^2} \quad (12)$$

$$l_B = \sqrt{(l_f - x_B)^2 + z_B^2} \quad (13)$$

Finally, the angles of  $\alpha$  and  $\beta$  are calculated from varied roll angle  $\phi_z$  as equations (14) and (15).

$$\alpha = \phi_x \cos \phi_z + \phi_y \sin \phi_z \quad (14)$$

$$\beta = -\phi_x \sin \phi_z + \phi_y \cos \phi_z \quad (15)$$

**Mechanical property and its evaluation**

(a) Movable area

Movable area of the head of the probe is mainly calculated with the lengths of the link of the pantograph. We defined the boundary whether solution of the inverse kinematics exists or not. The distance between two slides is adjustable but it is fixed to  $l_f=650$ [mm] because of the width of a general stretcher for emergency use. Figure 8 shows a theoretical movable area in  $x$ - $z$  plane using  $l_1=208$ [mm] and  $l_2=168$ [mm]. The area forms as axial cross section of human body and covers the shape of a normal adult patient where  $(x, z)=(0, 0)$  is defined as the middle of two slides on the surface of bed. Also actual movable area is measured and plotted on the same graph. The shape of the trajectory reveals an ellipse but includes two notches at  $z=250$ [mm] that means interference between the slide and the gimbals. Movable length in  $y$ -direction is 300[mm] which is defined by the  $y$ -length of the slide and independent to the pantograph part.

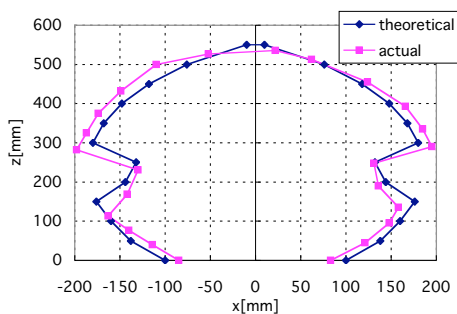


Figure 8: Movable area of the head of the probe in  $x$ - $z$  plane

(b) Position and angle precision

Figure 9 and 10 show the relation between the operated command and actual response of the position in  $x$ -directional translation by the pantograph and the roll angle by twist motion, respectively. The precision in  $x$ -directional translation is about 12[mm] inside movable area. It is allowable in echography but must be considered that surface of patient abdomen is not mathematical plane. The precision of the roll angle rotation is less than 2[deg] where absolute roll angle is within 45[deg]. Otherwise, however, it is not reliable with maximum error of 10[%].

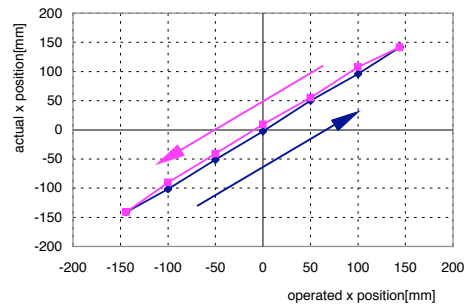


Figure 9: Comparison of the command and actual position in  $x$ -directional translation

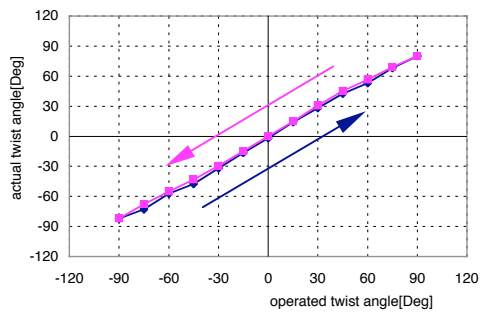


Figure 10: Comparison of the command and actual roll angle

(c) Performance of twist motion

Figure 11 shows a response of the roll angle rotation, which is produced by the twist motion of the pantograph and the slides. To rotate 15[deg], it took more than 1[sec] because  $y$ -positions of the slides are determined with rotary encoders which speed is reduced quarterly from the original actuator. It is allowable for diagnosis of echography but should be improved faster. The response in  $x$ - and  $z$ -direction translation in 50[mm] is less than 1[sec] which thought to be comfortable response for a physician.

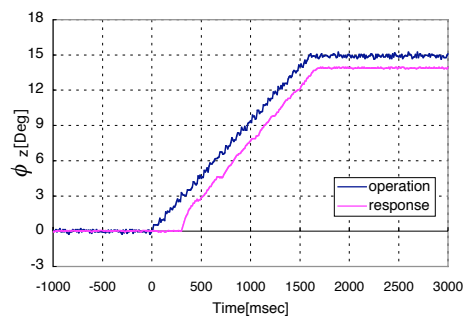


Figure 11: Response of the roll angle rotation

## Contact force detection

We also considered to detect contact force on body surface not to damage the patient. Miniature strain gauge was pasted on the middle of each longer link of the pantograph. When the head of the probe contacts on body surface of the patient, restitution force to the probe is sensed as strain of the link, which is shown in Figure 12. To enhance the sensitivity of the strain gauge, the link is slitted slightly on the opposite face of the strain gauge. To measure contact force, we have calibrated output of the strain gauge to restitution force. It must be always monitored during examination because normal volunteers felt pain if contact force exceeds 1[kgf].

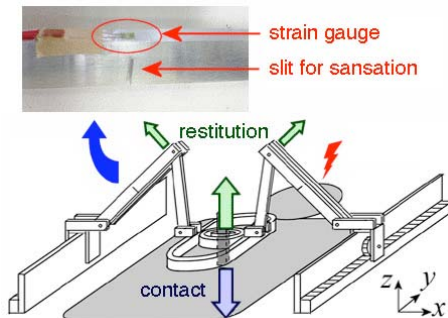


Figure 12: Location of strain gauges to detect contact force on body surface

## Results of remote control experiment

We also have developed software to control the robot via network using socket transportation of TCP/IP. Figure 13 shows a scene of experience with 100[Mbps] of campus LAN. The control device is seen in the right, which is especially developed for tele-echography by using parallel wire drive system[7] and is able to produce virtual restitution force to the hand of the physician. Minimum delay time was 0.5[sec] on the best condition of software.

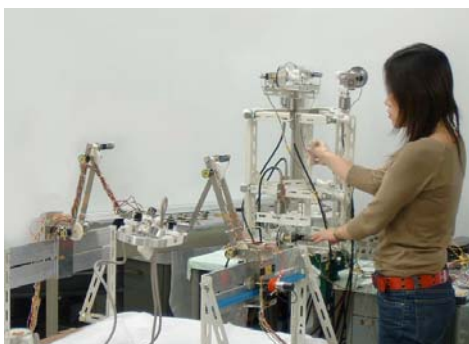


Figure 13: A scene of remote control experiment

Figure 14 shows a scene of experience with a normal male volunteer under the robot. The contact force on body surface was calculated and transferred to the control device. The physician performed to obtain echograms as her desire without any dangerous situation. Total weight of the robot is 2.0[kg] and that made the volunteer not feel any discomfort.

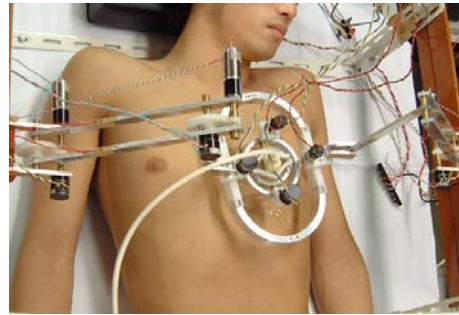


Figure 14: A scene of the robot mounted on a volunteer

## Conclusions

We have developed and experimented a twist pantograph mechanism of ultrasound probe for robotic tele-echography. The total mechanism is improved to be slimmed from the previous one and to be easily carried with the patient. Though the performance should be improved, precision of three-dimensional position and angle of the probe is reliable inside the movable area which covers almost body surface. We have confirmed the robot to realize robotic tele-echography in a narrow space as even in an emergency vehicle.

## Acknowledgements

We would like to express special thanks to our laboratory members, Ms. Yukari Nomoto and Mr. Hiroki Watanabe who supported the remote control experiment.

## References

- [1] A.Vilchis, J.Troccaz, P.Cinquin, K.Masuda and F.Pellissier: "A new robot architecture for tele-echography," *IEEE Transaction on Robotics and Automation*, Vol.19, No.5, 2003, pp.922-927
- [2] P.Abolmaesumi, S.E.Salcudean, W.H.Zhu, M.Sirouspour and S.DiMaio: "Image-guided control of a robot for medical ultrasound," *IEEE Transaction on Robotics and Automation*, Vol.18, No.1, 2002, pp.11-23
- [3] M.Mitsuishi, S.Warisawa, T.Tsuda, T.Higuchi, N.Koizumi, H.Hashizume and K.Fujiwara: "Remote ultrasound diagnosis system," *Proc. IEEE Int. Conf. Robotics & Automation*, 2001, pp.1567-1574
- [4] A.Gourdon, P.Poignet, G.Poisson, Y.Pamantier and P.March: "Master-slave robotic system for ultrasound scanning," *Proc. Eur. Medical & Biological Engineering Conf.*, Vol.II, 1999, pp.1116-1117
- [5] K.Masuda, E.Kimura, N.Tateishi and K.Ishihara: "Three dimensional motion mechanism of ultrasound probe and its application for tele-echography system," *Proc. IEEE Int. Conf. Intelligent Robots & Systems*, 2001, pp.1112-1116
- [6] K.Masuda, E.Kimura, N.Tateishi and K.Ishihara: "Robotic remote diagnosis system of echography for home care in the next generation," *Proc. 2nd Eur. Medical & Biological Engineering Conf.*, Vol.II, 2002, pp.1370-1371
- [7] Y.Nomoto and K.Masuda: "Development of parallel wire drive system for a control device in tele-echography," *Joint Conf. Automatic Control Eng.*, 2004, CD-ROM [in Japanese]